Doubly Cabibbo-suppressed decays of antitriplet charmed baryons

Guanbao Meng,[a] **Sam Ming-Yin Wong**[b] **and Fanrong Xu**[a,1]

[a]*Department of Physics, Jinan University,*
Guangzhou 510632, People's Republic of China

[b]*Department of Physics, National Taiwan University,*
Taipei 10617, Republic of China

E-mail: guanbaomeng@stu2018.jnu.edu.cn, D08222001@ntu.edu.tw,
fanrongxu@jnu.edu.cn

ABSTRACT: Doubly Cabibbo-suppressed (DCS) nonleptonic weak decays of antitriplet charmed baryons are studied systematically in this work. The factorizable and nonfactorizable contributions can be classified explicitly in the topological-diagram approach and treated separately. In particular, the evaluation of nonfactorizable terms is based on the pole model in conjunction with current algebra. All three types of relevant nonperturbative parameters contributing factorizable and nonfactorizable terms are estimated in the MIT bag model. Branching fractions of all the DCS decays are predicted to be of order $10^{-4} \sim 10^{-6}$. In particular, we find that the three modes $\Xi_c^+ \to \Sigma^+ K^0, \Sigma^0 K^+$ and $\Xi_c^0 \to \Sigma^- K^+$ are as large as $(1 \sim 2) \times 10^{-4}$, which are the most promising DCS channels to be measured. We also point out that the two DCS modes $\Xi_c^+ \to \Sigma^+ K^0$ and $\Xi_c^0 \to \Sigma^0 K^0$ are possible to be distinguished from $\Xi_c^+ \to \Sigma^+ K_S$ and $\Xi_c^0 \to \Sigma^0 K_S$. The decay asymmetries for all the channels with a kaon in their final states are found to be large in magnitude and negative in sign.

KEYWORDS: Phenomenological Models, QCD Phenomenology

ARXIV EPRINT: 2005.12111

---

[1]Corresponding author.

Contents

1 Introduction

It is known that weak decays dominate the decays of antitriplet charmed baryons, consisting of Λ_c^+, Ξ_c^0 and Ξ_c^+. Since four quarks get involved in weak decays of the antitriplet charmed baryons at tree level, we usually classify the weak decays into Cabibbo-favored (CF), singly Cabibbo-suppressed (SCS) and doubly Cabibbo-suppressed (DCS) modes according to the power of $\sin\theta_c \cos\theta_c$, where θ_c is the Cabibbo angle.

Recently, some progresses have been made in the experimental study of charm baryons. First, both Belle [1] and BESIII [2] have measured the absolute branching fraction of the decay $\Lambda_c^+ \to pK^-\pi^+$, leading to a new average of $(6.28 \pm 0.32)\%$ for this benchmark mode quoted by the Particle Data Group (PDG) [3]. The measurement of $\Lambda_c^+ \to p\pi^0, p\eta$ [4] performed in BESIII indicated that SCS decays are ready to access. Belle has also made some new developments in the study of Ξ_c^0 and Ξ_c^+, the two other singly charmed baryons in the antitriplet. By using a data set comprising $(772 \pm 11) \times 10^6$ $B\bar{B}$ pairs collected at $\Upsilon(4S)$ resonance, Belle was able to measure the branching ratios of charged and neutral Ξ_c decays [5, 6]. In addition to the discovery of doubly charmed baryon, recently LHCb also make a significant contribution in singly charmed baryon. Three new Ξ_c^0 baryon states

have been observed through their decay into $\Lambda_c^+ K^-$ [7]. In particular, BESIII recently has published a white paper on its future prospect [8], indicating that the measurement of DCS decays is also anticipated.

In recent theoretical studies, two main approaches have been adopted. In one methodology, connections among various decay amplitudes can be established based on SU(3) flavor symmetry. Then by taking a global fit to the existing experimental data as inputs, more channels can be predicted [10] (update results can be referred to [11]). Another new attempt has also been proposed by fitting topological diagrams and some predictions are also given [12]. The second approach to study charmed baryon weak decays is relying on model estimation, with which dynamics at the quark level can be revealed. To understand the underlying dynamical mechanism in hadronic weak decays, one may draw the topological diagrams according to the hadron's content [13]. In charmed baryon decays, nonfactorizable contributions from W-exchange or inner W-emission diagrams play an essential role and they cannot be neglected, in contrast with the negligible effects in heavy meson decays. To estimate the nonfactorizable effects in charmed baryon decays, various techniques were developed in the 1990s , including relativistic quark model (RQM) [14, 15], pole model [16, 18, 19] and current algebra [18, 20]. And recently an estimation of Λ_c^+ weak decays based on nonrelativistic constitutent quark model has been carried out [29].

Our estimation of nonfactorizable contribution will be based on the pole model. In the pole model, important low-lying $1/2^+$ and $1/2^-$ states are usually considered under the pole approximation. In the decay with a pseudoscalar in the final state, $\mathcal{B}_c \to \mathcal{B}' + P$, the nonfactorizable S- and P-wave amplitudes are dominated by $1/2^-$ low-lying baryon resonances and $1/2^+$ ground state baryons, respectively. The S-wave amplitude can be further reduced to current algebra in the soft-pseudoscalar limit. That is, the evaluation of the S-wave amplitude does not require the information of the troublesome negative-parity baryon resonances which are not well understood in the quark model. The methodology was developed and applied in the earlier work [18]. Our work is hence based on pole model in conjunction with current algebra. In our previous works, we have systematically studied weak decays of antitriplet charmed baryons [25, 26], the only weak decaying baryon in sextet Ω_c [28] and doubly charmed baryons [27]. It turns out if the S-wave amplitude is evaluated in the pole model or in the covariant quark model and its variant, the decay asymmetries for both $\Lambda_c^+ \to \Sigma^+ \pi^0$ and $\Sigma^0 \pi^+$ were always predicted to be positive, while it was measured to be $-0.45 \pm 0.31 \pm 0.06$ for $\Sigma^+ \pi^0$ by CLEO [21]. In contrast, current algebra always leads to a negative decay asymmetry for aforementioned two modes: -0.49 in [18], -0.31 in [20], -0.76 in [22] and -0.47 in [23]. The issue with the sign of $\alpha(\Lambda_c^+ \to \Sigma^+ \pi^0)$ was finally resolved by BESIII. The decay asymmetry parameters of $\Lambda_c^+ \to \Lambda \pi^+, \Sigma^0 \pi^+, \Sigma^+ \pi^0$ and pK_S were recently measured by BESIII [24], for example, $\alpha(\Lambda_c^+ \to \Sigma^+ \pi^0) = -0.57 \pm 0.12$ was obtained. Hence, the negative sign of $\alpha(\Lambda_c^+ \to \Sigma^+ \pi^0)$ measured by CLEO is nicely confirmed by BESIII. This is one of the strong reasons why we adapt current algebra to work out parity-violating amplitudes. For the antitriplet charmed baryon, the calculations for CF and SCS modes have been completed [25, 26]. In this paper, with the prospect from experiments indicated by of BESIII, we will continue completing the remaining piece, DCS decays of antitriplet charmed baryons.

This paper is organized as follows. In section 2 we will set up the formalism for evaluating branching fractions and up-down decay asymmetries, including contributions from both factorizable and nonfactorizable terms. Numerical results are presented in section 3. A conclusion will be given in section 4. In appendix A, we summarize all involved non-perturbative quantities calculated in MIT bag model, including baryon transition form factors, baryon matrix elements and the axial-vector form factors.

2 Theoretical framework

In this section, we will first introduce the generic kinematics of two-body hadronic decays. Then in the topological-diagram approach, factorizable and nonfactorizable amplitudes can be classified explicitly [17, 18]. The further calculation of the two parts of contributions are treated separately. For the factorizable amplitudes we evaluate them within naive factorization, while the pole model associated with current algebra technique is adopted in the calculation of nonfactorizable amplitudes.

2.1 Kinematics

Without loss of generality, the amplitude for the decay of an initial baryon $\mathcal{B}_i$ into a final baryon $\mathcal{B}_f$ and a pseudoscalar meson P can be parametrized as

$$M(\mathcal{B}_i \to \mathcal{B}_f P) = i\bar{u}_f(A - B\gamma_5)u_i, \tag{2.1}$$

where A and B stand for S- and P-wave amplitude, respectively. Both the two amplitudes contribute to the decay width and up-down decay asymmetry, giving

$$\Gamma = \frac{p_c}{8\pi}\left[\frac{(m_i + m_f)^2 - m_P^2}{m_i^2}|A|^2 + \frac{(m_i - m_f)^2 - m_P^2}{m_i^2}|B|^2\right],$$
$$\alpha = \frac{2\kappa\mathrm{Re}(A^*B)}{|A|^2 + \kappa^2|B|^2}, \tag{2.2}$$

where κ is defined as $\kappa = p_c/(E_f + m_f) = \sqrt{(E_f - m_f)/(E_f + m_f)}$ and p_c is the three-momentum in the rest frame of the mother particle. Obviously for the magnitude of decay width the contribution from S-wave amplitude is larger than the P-wave one up to a factor of $[(m_i + m_f)^2 - m_P^2]/[(m_i - m_f)^2 - m_P^2]$, while the sign of decay asymmetry is determined by the relative sign between A and B.

The S- and P- wave amplitudes of the two-body decay generally receive both factorizable and nonfactorizable contributions, giving

$$A = A^{\mathrm{fac}} + A^{\mathrm{nf}}, \quad B = B^{\mathrm{fac}} + B^{\mathrm{nf}}. \tag{2.3}$$

The nonfactorizable amplitudes, denoted as A^{nf} and B^{nf}, play an essential role in the decays of charmed baryon and hence cannot be ignored. This feature also differs from the situation in bottom baryon decays. The calculation of nonfactorizable amplitudes is a non-easy task and will be tackled in the following context.
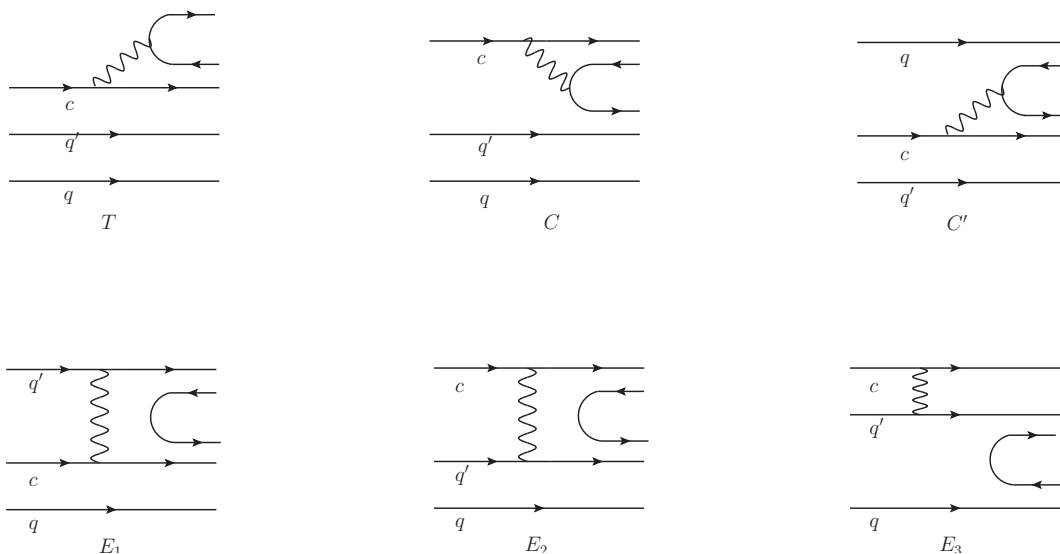
Figure 1. Topological diagrams contributing to antitriplet charmed baryons decays: external W-emission T, internal W-emission C, inner W-emission C', W-exchange diagrams E_1, E_2 and E_3.

2.2 Topological diagrams

The topological-diagram approach has been applied successfully in charmed meson decays. Various topological diagrams can be extracted from Cabibbo-favored (CF) channels. Then assuming SU(3) symmetry, we can use them to predict branching fractions of singly Cabibbo-suppressed (SCS) and doubly Cabibbo-suppressed (DCS) decays. Moreover, topological amplitudes allow to predict tree-induced CP violation as the information of strong phases can also be extracted. This is the power of the topological approach. For the charmed baryon decays, the application of the topological-diagram scheme was proposed and systematically summarized by Chau, Cheng and Tseng more than two decades ago [13]. However, there are not adequate data on branching fractions and decay asymmetries of charmed baryon decays to enable us extracting the topological diagrams. Nevertheless, we can still make use of the topological diagrams to classify the decay amplitudes into the factorizable and nonfactorizable ones.

For the weak decays $\mathcal{B}_c \to \mathcal{B} + P$ ($\mathcal{B}$ is baryon octet) of interest in this work, the relevant topological diagrams[1] are the external W-emission T, the internal W-emission C, the inner W-emission C', and the W-exchange diagrams E_1, E_2 and E_3 as depicted in figure 1. Among them, T and C are factorizable, while C' and W-exchange diagrams give nonfactorizable contributions. The relevant topological diagrams for DCS decay modes of antitriplet charm baryons are shown in table 1.

From table 1 we notice that (i) among all the DCS decays of antitriplet charmed baryons, there is no purely factorizable mode, (ii) the decays containing pion or η in their

---

[1]In principle, penguin diagrams can show up and give their contribution. However, in the evaluation of branching fractions and decay asymmetries in current work, they are considered to give sub-leading contributions and hence omitted in figure 1. One should keep in mind that these diagrams should play an important role in the calculation of CP violation.

Ξ_c^+	Contributions	Ξ_c^0	Contributions	Λ_c^+	Contributions
$\Xi_c^+ \to p\eta$	C', E_1, E_2, E_3	$\Xi_c^0 \to \Sigma^- K^+$	T, E_1	$\Lambda_c^+ \to pK^0$	C, C'
$\Xi_c^+ \to p\pi^0$	E_1, E_2, E_3	$\Xi_c^0 \to n\eta$	C', E_1, E_2, E_3	$\Lambda_c^+ \to nK^+$	T, C'
$\Xi_c^+ \to n\pi^+$	E_1, E_3	$\Xi_c^0 \to n\pi^0$	E_1, E_2, E_3		
$\Xi_c^+ \to \Sigma^0 K^+$	T, C', E_1, E_3	$\Xi_c^0 \to \Sigma^0 K^0$	C, C', E_2, E_3		
$\Xi_c^+ \to \Lambda^0 K^+$	T, C', E_1, E_3	$\Xi_c^0 \to \Lambda^0 K^0$	C, C', E_2, E_3		
$\Xi_c^+ \to \Sigma^+ K^0$	C, E_2	$\Xi_c^0 \to p\pi^-$	E_2, E_3		

Table 1. Topological diagrams contributing to DCS modes of two-body weak decays $\mathcal{B}_c \to \mathcal{B}P$, where $\mathcal{B}$ is a baryon octet and P is a pseudoscalar meson.

final states receive purely nonfactorizable contributions, and (iii) the modes containing kaon receive both factorizable and nonfactorizable contributions.

2.3 Factorizable amplitudes

In the frame of topological diagrams, the external W-emission T and internal W-emission C represent factorizable contributions. Strictly speaking, there are also nonfactorizable effects in the two diagrams. However, these nonfactorizable effects can be absorbed by an effective N_c in the effective Wilson coefficients, and the value of N_c can be extracted from the data. In that sense, the form of naive factorization can be kept and hence T and C can be classified into factorizable ones.

The effective Hamiltonian to describe the DCS decays of antitriplet charmed baryons is

$$\mathcal{H}_{\text{eff}} = \frac{G_F}{\sqrt{2}} V_{cd} V_{us}^* (c_1 O_1 + c_2 O_2) + H.c., \tag{2.4}$$

where the four-quark operators are given by

$$O_1 = (\bar{u}s)(\bar{d}c), \quad O_2 = (\bar{u}c)(\bar{d}s), \tag{2.5}$$

while the abbreviated notation in four-quark operators is defined as $(\bar{q}_1 q_2) \equiv \bar{q}_1 \gamma_\mu (1-\gamma_5) q_2$. The Wilson coefficients to the leading order are given as $c_1 = 1.346$ and $c_2 = -0.636$ at $\mu = 1.25\,\text{GeV}$ and $\Lambda_{\overline{\text{MS}}}^{(4)} = 325\,\text{MeV}$ [32]. Considering the mixing of operators, it is more convenient to introduce effective Wilson coefficients $a_1 = c_1 + \frac{c_2}{N_c}$ and $a_2 = c_2 + \frac{c_1}{N_c}$ where N_c is the number of colors. Topological diagrams contain all the final state interactions and in principle should also include non-factorizable contributions. However, it turns out in charm physics such effect is small. In order to incorporate the small non-factorizable effects we furthermore define an effective N_c and its value can be extracted from the experimental data. A recent measurement of $\mathcal{B}(\Lambda_c \to p\phi) = (1.04 \pm 0.21) \times 10^{-3}$ by BESIII [4], which receives purely factorizable contribution, indicates $N_c^{\text{eff}} \approx 7$, and hence we have $a_1 = 1.26$ and $a_2 = -0.45$ [25].

Now under naive factorization the amplitude can be written down as

$$M = \langle P\mathcal{B}|\mathcal{H}_{\text{eff}}|\mathcal{B}_c\rangle = \begin{cases} \dfrac{G_F}{\sqrt{2}} V_{cd} V_{us}^* a_1 \langle P|(\bar{u}s)|0\rangle \langle \mathcal{B}|(\bar{d}c)|\mathcal{B}_c\rangle, \ P = K^+, \\[2ex] \dfrac{G_F}{\sqrt{2}} V_{cd} V_{us}^* a_2 \langle P|(\bar{s}d)|0\rangle \langle \mathcal{B}|(\bar{u}c)|\mathcal{B}_c\rangle, \ P = K^0, \end{cases} \tag{2.6}$$

where a_1 corresponds to charged kaon while a_2 characterizes the amplitude with neutral kaon final state. In terms of the decay constants

$$\langle K(q)|\bar{s}\gamma_\mu(1-\gamma_5)d|0\rangle = if_K q_\mu \tag{2.7}$$

and the form factors defined by

$$\langle \mathcal{B}(p_2)|\bar{c}\gamma_\mu(1-\gamma_5)u|\mathcal{B}_c(p_1)\rangle = \bar{u}_2\left[f_1(q^2)\gamma_\mu - f_2(q^2)i\sigma_{\mu\nu}\frac{q^\nu}{M} + f_3(q^2)\frac{q_\mu}{M}\right. \tag{2.8}$$
$$\left. - \left(g_1(q^2)\gamma_\mu - g_2(q^2)i\sigma_{\mu\nu}\frac{q^\nu}{M} + g_3(q^2)\frac{q_\mu}{M}\right)\gamma_5\right]u_1,$$

with the momentum transfer $q = p_1 - p_2$, we obtain the amplitude

$$M(\mathcal{B}_c \to \mathcal{B}P) = i\frac{G_F}{\sqrt{2}}a_{1,2}V_{us}^*V_{cd}f_P\bar{u}_2(p_2)\left[(m_1-m_2)f_1(q^2)+(m_1+m_2)g_1(q^2)\gamma_5\right]u_1(p_1). \tag{2.9}$$

The contributions from the form factors f_3 and g_3 can be neglected for the similar reasons in the case of CF and CSC decays [26]. Hence the factorizable contributions to A and B terms finally read

$$A^{\text{fac}} = \frac{G_F}{\sqrt{2}}a_{1,2}V_{us}^*V_{cd}f_P(m_{\mathcal{B}_c} - m_{\mathcal{B}})f_1(q^2),$$
$$B^{\text{fac}} = -\frac{G_F}{\sqrt{2}}a_{1,2}V_{us}^*V_{cd}f_P(m_{\mathcal{B}_c} + m_{\mathcal{B}})g_1(q^2). \tag{2.10}$$

The factorizable amplitudes only appear in the modes containing kaon, and the choice of a_i is determined by the electric charge of final states kaon, see eq. (2.6).

The size of the factorizable amplitudes, together with the nonfactorizable ones, determines the branching fractions and decay asymmetries. Meanwhile its sign also plays a crucial role, which tells whether the interference with non-factorizable ones is destructive or constructive. In this work, the evaluation of baryon transition form factors f_1 and g_1 is carried out within the MIT bag model in the static limit. The exact calculated results for form factors are summarized in appendix A.1, where we first show the detailed results in the zero recoil limit $q^2 = (m_i - m_f)^2$ and then a further correction to $q^2 = m_P^2$ is made.

2.4 Nonfactorizable amplitudes

Nonfactorizable amplitudes give critical contributions in charmed baryon decays. In the topological-diagram approach, the three types of diagrams C', E_1, E_2 are classified to depict nonfactorizable contributions.[2] Various methods have been developed to study nonfactorizable contribution, here we keep on working in the pole model. There are two kinds of pole diagrmas in the pole model approximation. A correspondence is made between topological and pole diagrams, in which C' maps to type (2) in figure 2 while E_1 and E_2 identically corresponds to type (1) and E_3 receives both pole contributions.

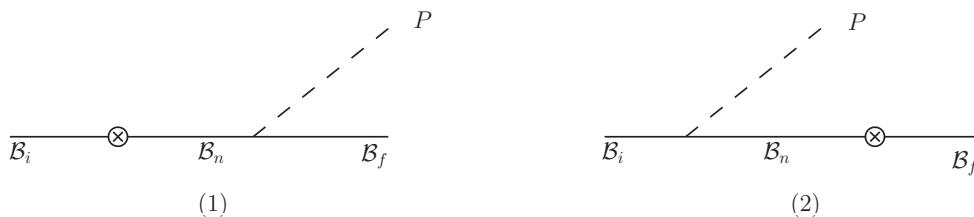[2]The contribution from E_3 will be discussed hereafter.

Figure 2. Pole diagrams for two-body charmed baryon hadronic decays with an initial baryon $\mathcal{B}_i$, a final baryon $\mathcal{B}_f$ and a final pseudoscalar meson P. The cross inserted in the straight line stands for weak interaction.

In the pole model, the general formula for S- and P-wave amplitudes can be extracted from a complete amplitude according to figure 2,

$$
A^{\text{pole}} = -\sum_{\mathcal{B}_n^*(1/2^-)} \left[\frac{g_{\mathcal{B}_f \mathcal{B}_n^* M} b_{n^* i}}{m_i - m_{n^*}} + \frac{b_{fn^*} g_{\mathcal{B}_n^* \mathcal{B}_i M}}{m_f - m_{n^*}} \right],
$$

$$
B^{\text{pole}} = \sum_{\mathcal{B}_n} \left[\frac{g_{\mathcal{B}_f \mathcal{B}_n M} a_{ni}}{m_i - m_n} + \frac{a_{fn} g_{\mathcal{B}_n \mathcal{B}_i M}}{m_f - m_n} \right], \tag{2.11}
$$

where g_{ijn} is the strong coupling among the pseudoscalar meson and two baryons, and the baryonic matrix elements a_{ij} and b_{ij} are defined as

$$
\langle \mathcal{B}_n | H | \mathcal{B}_i \rangle = \bar{u}_n (a_{ni} + b_{ni} \gamma_5) u_i, \qquad \langle \mathcal{B}_i^*(1/2^-) | H | \mathcal{B}_j \rangle = \bar{u}_{i*} b_{i^* j} u_j. \tag{2.12}
$$

To estimate the S-wave amplitudes in the pole model is a difficult and nontrivial task as it involves the matrix elements and strong coupling constants of $1/2^-$ baryon resonances which is less known [17]. Nevertheless, provided a soft emitted pseudoscalar meson,[3] the intermediate excited baryons can be summed up, leading to a commutator term

$$
A^{\text{com}} = -\frac{\sqrt{2}}{f_{P^a}} \langle \mathcal{B}_f | [Q_5^a, H_{\text{eff}}^{\text{PV}}] | \mathcal{B}_i \rangle = \frac{\sqrt{2}}{f_{P^a}} \langle \mathcal{B}_f | [Q^a, H_{\text{eff}}^{\text{PC}}] | \mathcal{B}_i \rangle, \tag{2.13}
$$

with the conserving charges

$$
Q^a = \int d^3x \, \bar{q} \gamma^0 \frac{\lambda^a}{2} q, \qquad Q_5^a = \int d^3x \, \bar{q} \gamma^0 \gamma_5 \frac{\lambda^a}{2} q. \tag{2.14}
$$

Likewise, the P-wave amplitude is reduced in the soft-meson limit to

$$
B^{\text{ca}} = \frac{\sqrt{2}}{f_{P^a}} \sum_{\mathcal{B}_n} \left[g_{\mathcal{B}_f \mathcal{B}_n}^A \frac{m_f + m_n}{m_i - m_n} a_{ni} + a_{fn} \frac{m_i + m_n}{m_f - m_n} g_{\mathcal{B}_n \mathcal{B}_i}^A \right], \tag{2.15}
$$

where the generalized Goldberger-Treiman relation,

$$
g_{\mathcal{B}' \mathcal{B} P^a} = \frac{\sqrt{2}}{f_{P^a}} (m_{\mathcal{B}} + m_{\mathcal{B}'}) g_{\mathcal{B}' \mathcal{B}}^A, \tag{2.16}
$$

has been applied. Our followup calculations will be based on eqs. (2.13) and (2.15) in the pole model under the soft meson approximation.

---

[3]In the condition of soft pseudoscalar meson, one can simplify calculation to avoid evaluation involving negative-parity $\frac{1}{2}^-$ intermediate baryons [25]. In principle, there will be a correction from large meson momentum, which will be shown in our future work. In practice, it has predicted a correct sign of the decay asymmetry for Cabibbo-allowed $\Lambda_c^+ \to \Sigma\pi$ and yields decay asymmetries for Cabibbo-suppressed modes in agreement with SU(3)-symmetry approach.

2.4.1 S-wave amplitudes

As shown in eq. (2.13), the nonfactorizable S-wave amplitude can be simplified into the commutator terms of conserving charge Q^a and the parity-conserving part of the Hamiltonian. Under SU(3) symmetry, the involved conserving charges in different decays are determined by final state mesons. In terms of commutators, the exact expressions for various S-wave amplitudes are:

$$A^{\mathrm{com}}(B_i \to B_f \pi^{\pm}) = \frac{1}{f_\pi} \langle B_f | [I_{\mp}, H_{\mathrm{eff}}^{PC}] | B_i \rangle,$$

$$A^{\mathrm{com}}(B_i \to B_f \pi^0) = \frac{\sqrt{2}}{f_\pi} \langle B_f | [I_3, H_{\mathrm{eff}}^{PC}] | B_i \rangle,$$

$$A^{\mathrm{com}}(B_i \to B_f \eta_8) = \sqrt{\frac{3}{2}} \frac{1}{f_{\eta_8}} \langle B_f | [Y, H_{\mathrm{eff}}^{PC}] | B_i \rangle,$$

$$A^{\mathrm{com}}(B_i \to B_f K^{\pm}) = \frac{1}{f_K} \langle B_f | [V_{\mp}, H_{\mathrm{eff}}^{PC}] | B_i \rangle,$$

$$A^{\mathrm{com}}(B_i \to B_f \overline{K}^0) = \frac{1}{f_K} \langle B_f | [U_+, H_{\mathrm{eff}}^{PC}] | B_i \rangle,$$

$$A^{\mathrm{com}}(B_i \to B_f K^0) = \frac{1}{f_K} \langle B_f | [U_-, H_{\mathrm{eff}}^{PC}] | B_i \rangle. \tag{2.17}$$

In particular, the octet component can be extracted from the mixing in η and η'

$$\eta = \cos\theta \eta_8 - \sin\theta \eta_0, \qquad \eta' = \sin\theta \eta_8 + \cos\theta \eta_0, \tag{2.18}$$

with $\theta = -15.4°$ [33, 34]. For the decay constant f_{η_8}, we shall follow [33, 34] to use $f_{\eta_8} = f_8 \cos\theta$ with $f_8 = 1.26 f_\pi$. As its conserving charge, hypercharge Y, we shall follow the convention $Y = B + S - C$ [25].

The calculation of commutators requires the information of baryon's behaviors under U, V, I symmetries. In this work, we still use the wave function conventions in our previous works [25–28], and especially their features under ladder operators can be found in appendix B of [26]. After a straightforward calculation of commutators, we obtain the S-wave amplitudes,

$$A^{\mathrm{com}}(\Xi_c^+ \to p\eta) = 0, \qquad\qquad A^{\mathrm{com}}(\Xi_c^+ \to p\pi^0) = 0,$$

$$A^{\mathrm{com}}(\Xi_c^+ \to n\pi^+) = \frac{1}{f_\pi} a_{p\Xi_c^+}, \qquad A^{\mathrm{com}}(\Xi_c^+ \to \Sigma^0 K^+) = -\frac{\sqrt{2}}{2f_K} a_{p\Xi_c^+},$$

$$A^{\mathrm{com}}(\Xi_c^+ \to \Lambda^0 K^+) = -\frac{\sqrt{6}}{2f_K} a_{p\Xi_c^+}, \qquad A^{\mathrm{com}}(\Xi_c^+ \to \Sigma^+ K^0) = -\frac{1}{f_K} a_{p\Xi_c^+},$$

$$A^{\mathrm{com}}(\Xi_c^0 \to n\pi^0) = 0, \qquad\qquad A^{\mathrm{com}}(\Xi_c^0 \to n\eta_8) = 0,$$

$$A^{\mathrm{com}}(\Xi_c^0 \to \Sigma^- K^+) = -\frac{1}{f_K} a_{n\Xi_c^0}, \qquad A^{\mathrm{com}}(\Xi_c^0 \to \Sigma^0 K^0) = \frac{\sqrt{2}}{2f_K} a_{n\Xi_c^0},$$

$$A^{\mathrm{com}}(\Xi_c^0 \to \Lambda^0 K^0) = -\frac{\sqrt{6}}{2f_K} a_{n\Xi_c^0}, \qquad A^{\mathrm{com}}(\Xi_c^0 \to p\pi^-) = \frac{1}{f_\pi} a_{n\Xi_c^0},$$

$$A^{\mathrm{com}}(\Lambda_c^+ \to pK^0) = \frac{1}{f_K} a_{p\Xi_c^+}, \qquad A^{\mathrm{com}}(\Lambda_c^+ \to nK^+) = -\frac{1}{f_K} a_{n\Xi_c^0}, \tag{2.19}$$

in which the quantities $a_{\mathcal{B}'\mathcal{B}}$ is defined in eq. (2.12). In particular, the vanishing S-wave amplitudes of the four modes decaying into $p\pi^0, p\eta, n\pi^0$ and $n\eta$ are due to the identical quantum numbers of initial and final baryons, specifically given as $I_3(n) = I_3(\Xi_c^0) = -\frac{1}{2}, I_3(p) = I_3(\Xi_c^+) = \frac{1}{2}$ for π^0 and $Y(n) = Y(\Xi_c^0) = 1, Y(p) = Y(\Xi_c^+) = 1$ for η. This natural consequence of current algebra, however, is too strong and a minor correction of current algebra will change the prediction dramatically, especially for the decay asymmetries. As for the two modes $\Xi_c^+ \to n\pi^+$ and $\Xi_c^0 \to p\pi^-$, a straightforward current algebra calculation yields two terms which cancel each other. As explained in the beginning of section 2.4, they correspond to E_3 which can be neglected. In eq. (2.19) current algebra results arise from E_1 for $\Xi_c^+ \to n\pi^+$ and E_2 for $\Xi_c^0 \to p\pi^-$. We will further illustrate the mechanism in the following section. A further estimation of baryon matrix elements $a_{\mathcal{B}'\mathcal{B}}$ in MIT bag model is carried out in appendix A.2.

2.4.2 P-wave amplitudes

According to eq. (2.15), the nonfactorizable P-wave amplitudes can be obtained by considering various intermediate states,

$$B^{\text{ca}}(\Xi_c^+ \to p\eta) = \frac{\sqrt{2}}{f_{\eta_8}} \left(a_{p\Xi_c^+} \frac{m_{\Xi_c^+} + m_{\Xi_c^+}}{m_p - m_{\Xi_c^+}} g_{\Xi_c^+ \Xi_c^+}^{A(\eta_8)} + a_{p\Xi_c'^+} \frac{m_{\Xi_c^+} + m_{\Xi_c'^+}}{m_p - m_{\Xi_c'^+}} g_{\Xi_c'^+ \Xi_c^+}^{A(\eta_8)} \right.$$
$$\left. + g_{pp}^{A(\eta_8)} \frac{m_p + m_p}{m_{\Xi_c^+} - m_p} a_{p\Xi_c^+} \right),$$

$$B^{\text{ca}}(\Xi_c^+ \to p\pi^0) = \frac{\sqrt{2}}{f_\pi} \left(g_{pp}^{A(\pi^0)} \frac{m_p + m_p}{m_{\Xi_c^+} - m_p} a_{p\Xi_c^+} \right),$$

$$B^{\text{ca}}(\Xi_c^+ \to n\pi^+) = \frac{1}{f_\pi} \left(g_{np}^{A(\pi^+)} \frac{m_n + m_p}{m_{\Xi_c^+} - m_p} a_{p\Xi_c^+} \right),$$

$$B^{\text{ca}}(\Xi_c^+ \to \Sigma^0 K^+) = \frac{1}{f_K} \left(g_{\Sigma^0 p}^{A(K^+)} \frac{m_{\Sigma^0} + m_p}{m_{\Xi_c^+} - m_p} a_{p\Xi_c^+} + a_{\Sigma^0 \Omega_c^0} \frac{m_{\Xi_c^+} + m_{\Omega_c^0}}{m_{\Sigma^0} - m_{\Omega_c^0}} g_{\Omega_c^0 \Xi_c^+}^{A(K^+)} \right),$$

$$B^{\text{ca}}(\Xi_c^+ \to \Lambda^0 K^+) = \frac{1}{f_K} \left(g_{\Lambda^0 p}^{A(K^+)} \frac{m_{\Lambda^0} + m_p}{m_{\Xi_c^+} - m_p} a_{p\Xi_c^+} + a_{\Lambda^0 \Omega_c^0} \frac{m_{\Xi_c^+} + m_{\Omega_c^0}}{m_{\Lambda^0} - m_{\Omega_c^0}} g_{\Omega_c^0 \Xi_c^+}^{A(K^+)} \right),$$

$$B^{\text{ca}}(\Xi_c^+ \to \Sigma^+ K^0) = \frac{1}{f_K} \left(g_{\Sigma^+ p}^{A(K^0)} \frac{m_{\Sigma^+} + m_p}{m_{\Xi_c^+} - m_p} a_{P\Xi_c^+} \right),$$

$$B^{\text{ca}}(\Xi_c^0 \to \Sigma^- K^+) = \frac{1}{f_K} \left(g_{\Sigma^- n}^{A(K^+)} \frac{m_{\Sigma^-} + m_n}{m_{\Xi_c^0} - m_n} a_{n\Xi_c^0} \right),$$

$$B^{\text{ca}}(\Xi_c^0 \to n\eta) = \frac{\sqrt{2}}{f_{\eta_8}} \left(a_{n\Xi_c^0} \frac{m_{\Xi_c^0} + m_{\Xi_c^0}}{m_n - m_{\Xi_c^0}} g_{\Xi_c^0 \Xi_c^0}^{A(\eta_8)} + a_{n\Xi_c'^0} \frac{m_{\Xi_c^0} + m_{\Xi_c'^0}}{m_n - m_{\Xi_c'^0}} g_{\Xi_c'^0 \Xi_c^0}^{A(\eta_8)} \right.$$
$$\left. + g_{nn}^{A(\eta_8)} \frac{m_n + m_n}{m_{\Xi_c^0} - m_n} a_{n\Xi_c^0} \right),$$

$$B^{\text{ca}}(\Xi_c^0 \to n\pi^0) = \frac{\sqrt{2}}{f_\pi} \left(g_{nn}^{A(\pi^0)} \frac{m_n + m_n}{m_{\Xi_c^0} - m_n} a_{n\Xi_c^0} \right),$$

$$B^{\mathrm{ca}}(\Xi_c^0 \to \Sigma^0 K^0) = \frac{1}{f_K} \left(g_{\Sigma^0 n}^{A(K^0)} \frac{m_{\Sigma^0} + m_n}{m_{\Xi_c^0} - m_n} a_{n\Xi_c^0} + a_{\Sigma^0 \Omega_c^0} \frac{m_{\Xi_c^0} + m_{\Omega_c^0}}{m_{\Sigma^0} - m_{\Omega_c^0}} g_{\Omega_c^0 \Xi_c^0}^{A(K^0)} \right),$$

$$B^{\mathrm{ca}}(\Xi_c^0 \to \Lambda^0 K^0) = \frac{1}{f_K} \left(g_{\Lambda^0 n}^{A(K^0)} \frac{m_{\Lambda^0} + m_n}{m_{\Xi_c^0} - m_n} a_{n\Xi_c^0} + a_{\Lambda^0 \Omega_c^0} \frac{m_{\Xi_c^0} + m_{\Omega_c^0}}{m_{\Lambda^0} - m_{\Omega_c^0}} g_{\Omega_c^0 \Xi_c^0}^{A(K^0)} \right),$$

$$B^{\mathrm{ca}}(\Xi_c^0 \to p\pi^-) = \frac{1}{f_\pi} \left(g_{pn}^{A(\pi^-)} \frac{m_p + m_n}{m_{\Xi_c^0} - m_n} a_{n\Xi_c^0} \right),$$

$$B^{\mathrm{ca}}(\Lambda_c^+ \to p K^0) = \frac{1}{f_K} \left(a_{p\Xi_c^+} \frac{m_{\Lambda_c^+} + m_{\Xi_c^+}}{m_p - m_{\Xi_c^+}} g_{\Xi_c^+ \Lambda_c^+}^{A(K^0)} + a_{p\Xi_c'^+} \frac{m_{\Lambda_c^+} + m_{\Xi_c'^+}}{m_p - m_{\Xi_c'^+}} g_{\Xi_c'^+ \Lambda_c^+}^{A(K^0)} \right),$$

$$B^{\mathrm{ca}}(\Lambda_c^+ \to n K^+) = \frac{1}{f_K} \left(a_{n\Xi_c^0} \frac{m_{\Lambda_c^+} + m_{\Xi_c^0}}{m_n - m_{\Xi_c^0}} g_{\Xi_c^0 \Lambda_c^+}^{A(K^+)} + a_{n\Xi_c'^0} \frac{m_{\Lambda_c^+} + m_{\Xi_c'^0}}{m_n - m_{\Xi_c'^0}} g_{\Xi_c'^0 \Lambda_c^+}^{A(K^+)} \right). \quad (2.20)$$

In general, the two types of non-perturbative parameters, $a_{\mathcal{B}\mathcal{B}'}$ and $g_{\mathcal{B}\mathcal{B}'}^{A(P)}$, can be calculated by Lattice QCD, QCD sum rule or quark models. The MIT bag model, as aforementioned, is taken in this work and the estimated results are shown explicitly in appendices A.2 and A.3.

3 Results and discussion

In this section, we first present the details of numerical results of relevant branching fractions and decay asymmetries. Specifically, we clarify the relation between modes with K_S final state, which are more concerned by experimentalists, and CF modes containing $\overline{K}^0$ as well as DCS modes with K^0. A comparison of theoretical predictions with other groups is also made in the end.

3.1 Numerical results

Based on analytical equations eq. (2.2) and relevant expressions for each component, now we shall numerically calculate branching fractions and up-down decay asymmetries. The decay asymmetries purely depend on S- and P-wave amplitudes while branching fractions rely on more parameters, lifetimes. In this work, the values of lifetime are taken as the new world averages (in units of 10^{-13} s)

$$\tau(\Lambda_c^+) = 2.03 \pm 0.02, \qquad \tau(\Xi_c^+) = 4.56 \pm 0.05, \qquad \tau(\Xi_c^0) = 1.53 \pm 0.02. \quad (3.1)$$

Especially note that the measured Ξ_c^0 lifetime by the LHCb is approximately 3.3 standard deviations larger than the old world average value [3].

All the channels with a kaon in the final states receive both factorizable and non-factorizable contributions. For the factorizable amplitudes A^{fac} and B^{fac}, their signs are co-determined by effective Wilson coefficients a_1, a_2 and FFs f_1, g_1. The flipped sign between $\Sigma^0 K^+$ and $\Lambda^0 K^+$ is due to the sign difference between FFs, sharing common effective Wilson coefficient a_1. And for the two modes $\Sigma^+ K^0$ and $\Lambda^0 K^+$, their FFs are both negative but differ from effective Wilson coefficients, hence their factorizable S-wave amplitudes are also with wrong sign. On the other side, the signs of nanfactorizable terms of the three

Modes	A^{fac}	A^{com}	A^{tot}	B^{fac}	B^{ca}	B^{tot}	$\mathcal{B}_{\mathrm{theo}}$	$\mathcal{B}_{\mathrm{expt}}$	α_{theo}
$\Xi_c^+ \to p\eta$	0	0	0	0	-0.51	-0.51	0.32	$-$	0
$\Xi_c^+ \to p\pi^0$	0	0	0	0	0.28	0.28	0.12	$-$	0
$\Xi_c^+ \to n\pi^+$	0	0.29	0.29	0	0.39	0.39	0.88	$-$	0.88
$\Xi_c^+ \to \Sigma^+ K^0$	-0.14	-0.24	-0.39	0.50	0.08	0.58	1.28	$-$	-0.79
$\Xi_c^+ \to \Sigma^0 K^+$	-0.28	-0.17	-0.45	1.00	0.06	1.05	2.26	$-$	-0.96
$\Xi_c^+ \to \Lambda^0 K^+$	0.15	-0.30	-0.15	-0.51	0.64	0.13	0.18	$-$	-0.54
$\Xi_c^0 \to p\pi^-$	0	0.29	0.29	0	0.39	0.39	0.30	$-$	0.88
$\Xi_c^0 \to n\pi^0$	0	0	0	0	-0.28	-0.28	0.04	$-$	0
$\Xi_c^0 \to n\eta$	0	0	0	0	-0.52	-0.52	0.11	$-$	0
$\Xi_c^0 \to \Sigma^- K^+$	-0.40	-0.24	-0.64	1.42	0.08	1.50	1.52	$-$	-0.96
$\Xi_c^0 \to \Sigma^0 K^0$	0.10	0.17	0.27	-0.35	-0.06	-0.41	0.22	$-$	-0.79
$\Xi_c^0 \to \Lambda^0 K^0$	0.05	-0.30	-0.25	-0.18	0.64	0.46	0.20	$-$	-0.92
$\Lambda_c^+ \to pK^0$	-0.13	0.24	0.11	0.40	-0.51	-0.11	0.04	$-$	-0.65
$\Lambda_c^+ \to nK^+$	0.36	-0.24	0.12	-1.13	0.51	-0.62	0.21	$-$	-0.77

Table 2. Amplitudes (in units of $10^{-2} G_F \mathrm{GeV}^2$), branching fractions (in units of 10^{-4}) and decay asymmetries α of DCS modes of weak decays $\mathcal{B}_c \to \mathcal{B}_f P$.

modes are the same for both S- and P-wave amplitudes. Thus with constructive interference, the predictions of branching fractions for the two modes $\Sigma^+ K^0$ and $\Sigma^0 K^+$ is one order of magnitude larger than $\Lambda^0 K^+$, which receive a destructive interference. The situation is similar in the case of Ξ_c^0 decays. However, for the two decaying modes of Λ_c^+, factorizable and nonfactorizable contributions to both S- and P-wave amplitudes have opposite sign thus a cancellation occurs, leading to the smaller magnitudes of the branching ratios of 10^{-5} or even 10^{-6}.[4] Among all the DCS decay modes, the three channels $\Xi_c^+ \to \Sigma^+ K^0$, $\Xi_c^+ \to \Sigma^0 K^+$ and $\Xi_c^0 \to \Sigma^- K^+$ are predicted to be most accessible by future experiments, as large as 10^{-4} in magnitude for their branching fractions. The decay asymmetries, on the other hand, are all predicted to be negative in sign and larger than 0.5 in magnitude.

The contribution from W-exchange diagram E_3 in figure 1 has been neglected throughout the whole calculation. This feature was first pointed out by Körner and Krämer [14] and argued by Zenczykowski [19] according to spin-flavor structure. A recent global fitting in terms of topological diagrams also indicates the smallness of E_3 [12]. By dropping E_3 contribution, which induces strong cancellations in both S- and P-wave amplitudes, the long-standing puzzle in $\Lambda_c^+ \to \Xi^0 K^+$ has been successfully resolved recently [26]. Hence in this work, we continue working in this scheme and find the two modes $\Xi_c^+ \to n\pi^+$ and $\Xi_c^0 \to p\pi^-$ are manifestly affected. A straightforward calculation of commutators in S-wave is subject to a strong cancellation between $a_{p\Xi_c^+}$ and $a_{n\Xi_c^0}$. Such a cancellation can be understood from the two pole diagrams corresponding to E_3. Due to the aforementioned reasons, E_3 can be neglected and hence the cancellation can be avoided. The

---

[4]If we adopt both the magnitude and sign of form factors calculated in Lattice QCD, shown in table 5, the predictions of the two modes will be enhanced as $\mathcal{B}(\Lambda_c^+ \to pK^0) = 1.2 \times 10^{-4}$, $\mathcal{B}(\Lambda_c^+ \to nK^+) = 4.54 \times 10^{-4}$.

remaining results then are obtained by taking into account another W-exchange diagram E_1 for $\Xi_c^+ \to n\pi^+$ and E_2 for $\Xi_c^0 \to p\pi^-$. Especially for the mode $\Xi_c^+ \to n\pi^+$, its branching fractions is predicted to be close to 1×10^{-4} and decay asymmetries are large in magnitude and positive in sign, which is possibly accessible by BESIII or Belle-II in the near future.

The topological diagrams have revealed that the modes containing a pion or η receive purely nonfactorizable contributions. Furthermore, the calculation in the soft-pseudoscalar limit indicates that the nonfactorizable S-wave of all modes with neutral pseudoscalar vanish. The identical quantum numbers (third-component of isospin or hypercharge) of initial and final baryons lead to vanishing baryon matrix elements of commutators, which is a natural consequence of current algebra. This feature of current algebra calculation, however, is less reliable for the four modes. At least a correction of current algebra result may induce an obvious different prediction to decay asymmetry. An exact pole model estimation will be carried out in our future work.

From the experimental point of view, the measured neutral kaon is actually K_S with its lifetime $\tau = 8.954 \times 10^{-11}$s. From the relation between $K_{S,L}$ and $K^0, \overline{K}^0$

$$
\begin{aligned}
K_S &= \frac{1}{\sqrt{2}} \left(\frac{1+\epsilon}{\sqrt{1+|\epsilon|^2}} K^0 + \frac{-1+\epsilon}{\sqrt{1+|\epsilon|^2}} \overline{K}^0 \right), \\
K_L &= \frac{1}{\sqrt{2}} \left(\frac{1+\epsilon}{\sqrt{1+|\epsilon|^2}} K^0 + \frac{1-\epsilon}{\sqrt{1+|\epsilon|^2}} \overline{K}^0 \right),
\end{aligned}
\tag{3.2}
$$

together with $|\epsilon| = (2.228 \pm 0.011) \times 10^{-3}$ [3], we can get

$$
\text{Br}(\mathcal{B}_c \to \mathcal{B} K_S) \approx \frac{1}{2}\text{Br}(\mathcal{B}_c \to \mathcal{B} K^0) + \frac{1}{2}\text{Br}(\mathcal{B}_c \to \mathcal{B} \overline{K}^0).
\tag{3.3}
$$

For the Λ_c^+ decays, it is interesting to notice that $\Lambda_c \to p\overline{K}^0$ is CF process with the predicted branching fraction 2.11×10^{-2} [26] while $\Lambda_c \to pK^0$ is DCS one with branching fraction 4×10^{-6} predicted in current work. This huge but natural difference between the two modes hence brings difficulty to extract the data of $\Lambda_c^+ \to pK^0$ from the measurement of $\Lambda_c^+ \to pK_S$ in BESIII. The similar situation occurs in the decays $\Xi_c^0 \to \Lambda^0\overline{K}^0$ and $\Xi_c^0 \to \Lambda^0 K^0$. Fortunately, there are two exceptions,

$$
\begin{aligned}
\text{Br}(\Xi_c^+ \to \Sigma^+\overline{K}^0) = 2 \times 10^{-3} \text{ (CF)}, \qquad \text{Br}(\Xi_c^+ \to \Sigma^+ K^0) = 1 \times 10^{-4} \text{ (DCS)}, \\
\text{Br}(\Xi_c^0 \to \Sigma^0\overline{K}^0) = 4 \times 10^{-4} \text{ (CF)}, \qquad \text{Br}(\Xi_c^0 \to \Sigma^0 K^0) = 2 \times 10^{-5} \text{ (DCS)},
\end{aligned}
\tag{3.4}
$$

in which the differences between CF (see [26]) and DCS modes are not dramatically huge. Thus it is hopeful to measure the two DCS modes, especially $\Xi_c^+ \to \Sigma^+ K^0$, when more data are accumulated. To be specific, we can also give predictions

$$
\text{Br}(\Xi_c^+ \to \Sigma^+ K_S) = 1.1 \times 10^{-3}, \quad \text{Br}(\Xi_c^0 \to \Sigma^0 K_S) = 2.1 \times 10^{-4},
\tag{3.5}
$$

which can be tested by Belle-II or BESIII in the near future.

Modes	Our work	Geng et al. [10, 11]	Zhao et al. [12]	Experiment
$\Xi_c^+ \to p\eta$	3.2(0)	$19.8 \pm 7.6(-0.58 \pm 0.12)$	16.6 ± 3.1	–
$\Xi_c^+ \to p\pi^0$	1.2(0)	$5.3 \pm 1.2(0.81 \pm 0.12)$	1.5 ± 1.5	–
$\Xi_c^+ \to n\pi^+$	8.8(0.88)	$10.7 \pm 2.4(0.81 \pm 0.12)$	5.2 ± 1.5	–
$\Xi_c^+ \to \Sigma^+ K^0$	12.8(-0.79)	$18.6 \pm 1.6(-0.96^{+0.11}_{-0.04})$	16.9 ± 5.4	–
$\Xi_c^+ \to \Sigma^0 K^+$	22.6(-0.96)	$12.1 \pm 0.6(-1.00^{+0.02}_{-0.0})$	7.2 ± 1.8	–
$\Xi_c^+ \to \Lambda^0 K^+$	1.8(-0.54)	$3.1 \pm 0.5(0.50 \pm 0.16)$	7.5 ± 1.9	–
$\Xi_c^0 \to n\eta$	1.1(0)	$6.6 \pm 2.5(-0.58 \pm 0.12)$	4.2 ± 0.8	–
$\Xi_c^0 \to n\pi^0$	0.4(0)	$1.8 \pm 0.4(0.81 \pm 0.12)$	3.3 ± 0.9	–
$\Xi_c^0 \to p\pi^-$	3.0(0.88)	$3.6 \pm 0.8(0.81 \pm 0.12)$	7.6 ± 2.0	–
$\Xi_c^0 \to \Lambda^0 K^0$	2(-0.92)	$0.9 \pm 0.3(0.00 \pm 0.33)$	2.4 ± 1.4	–
$\Xi_c^0 \to \Sigma^0 K^0$	2.2(-0.79)	$3.1 \pm 0.3(-0.96^{+0.11}_{-0.04})$	2.3 ± 1.4	–
$\Xi_c^0 \to \Sigma^- K^+$	15.2(-0.96)	$8.1 \pm 0.4(-1.00^{+0.02}_{-0})$	5.5 ± 0.7	–
$\Lambda_c^+ \to pK^0$	0.4(-0.65)	$0.8 \pm 1.1(0.97^{+0.03}_{-0.12})$	3.7 ± 1.1	–
$\Lambda_c^+ \to nK^+$	2.1(-0.77)	$0.5 \pm 0.2(-0.61^{+0.76}_{-0.39})$	1.4 ± 0.5	–

Table 3. Comparison with other works for branching fractions in unit of 10^{-5} and decay asymmetries shown in parentheses.

3.2 Comparison with other works

Weak decays of charmed baryons have attracted many interests in recent time. Based on SU(3) flavor symmetry in theory and taking measured branching fractions and asymmetries as inputs, predictions of more branching fractions and decay asymmetries can be obtained in a global fitting picture [10, 11]. A recent new exploration by parameterizing topological diagrams with independent parameters also provides another set of predictions of branching fractions [12]. In this part a comparison with these groups is made and shown in table 3.

There are some common features for the three groups relying on different approaches. First the branching fractions of DCS decays are all ranged in $10^{-6} \sim 10^{-4}$. Especially for the decays $\Xi_c^+ \to \Sigma^+ K^0$, $\Xi_c^+ \to \Sigma^0 K^+$ and $\Xi_c^0 \to \Sigma^- K^+$, all the three groups agree that their branching fraction are of $(1 \sim 2) \times 10^{-4}$ and with large and negative decay asymmetries, which is highly accessible by Belle-II or BESIII in the near future. For the two modes $\Xi_c^+ \to n\pi^+$ and $\Xi_c^0 \to p\pi^-$, not only their branching fractions agree well for the three groups, but also the size as well as the sign of decay asymmetries can be confirmed by two independent groups. The consistent predictions for both branching ratios and decay asymmetries of $\Xi_c^+ \to n\pi^+$ and $\Xi_c^0 \to p\pi^-$, on the other hand, confirms our treatment by neglecting E_3. The size of $\Lambda_c^+ \to nK^+$, however, are of $(1 \sim 2) \times 10^{-5}$ in magnitude and also with large negative asymmetry. It is known that BESIII can reconstruct a neutron final state. With more data accumulated after its upgrade, this channel could possibly be measured [8].

There are also some disagreement in the three modes $\Xi_c^+ \to \Lambda^0 K^+$, $\Xi_c^0 \to \Lambda^0 K^0$ and $\Lambda_c^+ \to pK^0$. Our prediction for the branching fractions of $\Xi_c^+ \to \Lambda^0 K^+$ and $\Lambda_c^+ \to pK^0$

are the smallest among all the three groups, while for $\Xi_c^0 \to \Lambda^0 K^0$ ours is close to the prediction in [12]. For the decay asymmetries, ours differ from [10, 11] for the signs in the two modes $\Xi_c^+ \to \Lambda^0 K^+$ and $\Lambda_c^+ \to p K^0$, and magnitude for the mode $\Xi_c^0 \to \Lambda^0 K^0$.

4　Conclusions

In this work we have studied the branching fractions and up-down decay asymmetries of DCS decays of antitriplet charmed baryons. In the topological-diagram approach, we can identify factorizable and nonfactorizable contributions in each process clearly. The calculation of factorizable and nonfactorizable terms in S- and P-wave amplitudes is carried out in separated ways. For the factorizable amplitudes, by defining an effective color number N_c encoded in effective Wilson coefficients, one can make use of naive factorization. To estimate nonfactorizable contribution, we work in the pole model for P-wave amplitudes and current algebra for S-wave ones. All the non-perturbative parameters, including baryon-baryon transition form factors, baryon matrix elements and axial-vector form factors, are evaluated within the MIT bag model throughout the whole calculations.

　　Some conclusions can be drawn from our analysis as follows.

- The decays $\Xi_c^+ \to \Sigma^+ K^0, \Sigma^0 K^+$ and $\Xi_c^0 \to \Sigma^- K^+$ are the most promising DCS channels to be measured as their branching fractions are predicted to be as large as $(1 \sim 2) \times 10^{-4}$, which agree with the other predictions based on different approaches. The decay asymmetries are found to be large in magnitude and negative in sign.

- For the decay channels containing K^0 in the final states, it is possible to extract $\Xi_c^+ \to \Sigma^+ K^0$ and $\Xi_c^0 \to \Sigma^0 K^0$ from data with K_S in the final states. However, the measurement of $\Lambda_c^+ \to p K^0$ and $\Xi_c^0 \to \Lambda^0 K^0$ in experiment is challenging.

- Predictions for the two modes $\Xi_c^+ \to n \pi^+, \Xi_c^0 \to p \pi^-$ agree well among three different groups, both for their branching fractions and decay asymmetries. Though with small but anticipated branching fraction of 10^{-5}, a further confirmation from experiment will be significant to clarify the dynamic mechanism at the quark level.

Acknowledgments

A　Model estimation of non-perturbative parameters

There are three types of non-perturbative quantities involved in charmed baryon decays: the baryon transition form factors contributing to factorizable amplitudes and baryon matrix elements as well as axial vector form factors contributing to non-factorizable amplitudes. In this work, the estimation of these parameters are carried out within the framework of the MIT bag model [30, 31].

modes	$f_1(q^2_{\max})$	$f_1(m_P^2)/f_1(q^2_{\max})$	$f_1(m_P^2)$	$g_1(q^2_{\max})$	$g_1(m_P^2)/g_1(q^2_{\max})$	$g_1(m_P^2)$
$\Xi_c^+ \to \Sigma^0 K^+$	$\frac{\sqrt{3}}{2}Y_1$	0.404	0.308	$\frac{\sqrt{3}}{2}Y_2$	0.568	0.378
$\Xi_c^+ \to \Lambda^0 K^+$	$-\frac{1}{2}Y_1$	0.338	-0.150	$-\frac{1}{2}Y_2$	0.515	-0.198
$\Xi_c^+ \to \Sigma^+ K^0$	$-\frac{\sqrt{6}}{2}Y_1$	0.401	-0.433	$-\frac{\sqrt{6}}{2}Y_2$	0.567	-0.534
$\Xi_c^0 \to \Sigma^- K^+$	$\frac{\sqrt{6}}{2}Y_1$	0.404	0.437	$\frac{\sqrt{6}}{2}Y_2$	0.570	0.536
$\Xi_c^0 \to \Sigma^0 K^0$	$\frac{\sqrt{3}}{2}Y_1$	0.401	0.306	$\frac{\sqrt{3}}{2}Y_2$	0.567	0.377
$\Xi_c^0 \to \Lambda^0 K^0$	$\frac{1}{2}Y_1$	0.336	0.148	$\frac{1}{2}Y_2$	0.514	0.198
$\Lambda_c^+ \to p K^0$	$-\frac{\sqrt{6}}{2}Y_1$	0.342	-0.369	$-\frac{\sqrt{6}}{2}Y_2$	0.519	-0.488
$\Lambda_c^+ \to n K^+$	$-\frac{\sqrt{6}}{2}Y_1$	0.342	-0.370	$-\frac{\sqrt{6}}{2}Y_2$	0.519	-0.489

Table 4. The calculated form factors in the MIT bag model at maximum four-momentum transfer squared $q^2 = q^2_{\max} = (m_i - m_f)^2$ and $q^2 = m_P^2$.

A.1 Baryon transition form factors

In the zero recoil limit where $q^2_{\max} = (m_i - m_f)^2$, FFs calculated in the MIT bag model [18] are given as

$$f_1^{\mathcal{B}_f \mathcal{B}_i}(q^2_{\max}) = \langle \mathcal{B}_f^\uparrow | b_{q_1}^\dagger b_{q_2} | \mathcal{B}_i^\uparrow \rangle \int d^3 \boldsymbol{r} \left(u_{q_1}(r) u_{q_2}(r) + v_{q_1}(r) v_{q_2}(r) \right),$$

$$g_1^{\mathcal{B}_f \mathcal{B}_i}(q^2_{\max}) = \langle \mathcal{B}_f^\uparrow | b_{q_1}^\dagger b_{q_2} \sigma_z | \mathcal{B}_i^\uparrow \rangle \int d^3 \boldsymbol{r} \left(u_{q_1}(r) u_{q_2}(r) - \frac{1}{3} v_{q_1}(r) v_{q_2}(r) \right), \tag{A.1}$$

where $u(r)$ and $v(r)$ are the large and small components, respectively, of the quark wave function in the bag model. The two quark flavors q_1, q_2 are determined by the meson content. The physical FFs which contribute to the factorizable amplitudes are actually located at energy scale $q^2 = m_P^2$, thus an evolution from different energy scale is necessary. Follow [35], the connections of FFs at different scale assuming a dipole q^2 dependence are

$$f_i(q^2) = \frac{f_i(0)}{(1 - q^2/m_V^2)^2}, \qquad g_i(q^2) = \frac{g_i(0)}{(1 - q^2/m_A^2)^2}, \tag{A.2}$$

where the corresponding $m_V = 2.01 \, \text{GeV}$, $m_A = 2.42 \, \text{GeV}$ for the $(c\bar{d})$ quark content, and $m_V = 2.11 \, \text{GeV}$, $m_A = 2.54 \, \text{GeV}$ for $(c\bar{s})$ quark content.

It is obvious that the FF at $q^2_{\max}$ is determined only by the baryons in initial and final states. However, its evolution with q^2 is governed by both the final-state meson and relevant quark content. This feature manifests in table 4, where the FFs calculated at $q^2_{\max}$ in the zero recoil limit are presented in the second and fifth columns. The auxiliary quantities $Y_{1,2}$ can be obtained from the calculation in MIT bag model, giving

$$Y_1 = 4\pi \int r^2 dr (u_u u_c + v_u v_c), \qquad Y_2 = 4\pi \int r^2 dr (u_u u_c - \frac{1}{3} v_u v_c). \tag{A.3}$$

The model parameters are adopted from [25] and references therein. Numerically, we have $Y_1 = 0.88, Y_1^s = 0.95, Y_2 = 0.77, Y_2^s = 0.86$, which are consistent with the corresponding

modes	FF	ours	MBM old	LFQM	RQM	CCQM	LCSR-I	LCSR-II	LQCD
			[36]	[37]	[38]	[39]	[40]	[41]	[42]
$\Lambda_c \to N$	f_1	-0.326	0.39	-0.513	0.627	0.470	-0.52 ± 0.02	$0.46^{+0.15}_{-0.11}$	0.672 ± 0.039
	g_1	-0.449	0.84	-0.443	0.433	0.414	—	$0.49^{+0.14}_{-0.11}$	0.602 ± 0.031
$\Xi_c^+ \to \Sigma^0$	f_1	0.272	0.37	0.359					
	g_1	0.347	0.62	0.307					
$\Xi_c^+ \to \Lambda$	f_1	-0.132	0.10	0.207					
	g_1	-0.182	0.23	0.177					
$\Xi_c^0 \to \Sigma^-$	f_1	0.386	0.53	0.507					
	g_1	0.492	0.88	0.434					

Table 5. A comparison of form factors calculated with different methods at $q^2 = 0$.

numbers in [18]. The evolution constants are shown in third and sixth columns. And in fourth and seventh columns, we list physical FFs.

We also compare our MIT bag model (MBM) estimation on form factors at $q^2 = 0$ with an old calculation in the same model [36] under monopole approximation, light-front quark model (LFQM) [37], relativistic quark model (RQM) [38], covariant confined quark model (CCQM) [39], light-cone sum rule (LCSR) [40, 41] as well as lattice QCD (LQCD) calculation [42], shown in table 5. So far $\Lambda_c \to N$ (N is a nucleon) attracts more attention and we hope more efforts can also be contributed on other channels. Taking $\Lambda_c \to N$ as an example, our estimation of f_1 is the smallest among all the groups, about 20% smaller than CCQM and a half of LQCD. But for the size of g_1, all the quark model estimations in 5 groups, except the old MBM calculation, are consistent and around 30% smaller than LQCD result. For the signs of f_1 and g_1, only the LFQM result[5] agrees with ours. We should emphasize here that the sign of form factors in our calculation is consistent with the one in non-factorizable terms as all the non-perturbative parameters are calculated in the same model with consistent conventions.

A.2 Baryon matrix elements

The baryonic matrix elements $a_{\mathcal{B}'\mathcal{B}}$ get involved both in S- and P-wave amplitudes. Their general expression in terms of the effective Hamiltonian eq. (2.4) is given by

$$a_{\mathcal{B}'\mathcal{B}} \equiv \langle \mathcal{B}' | \mathcal{H}_{\text{eff}}^{\text{PC}} | \mathcal{B} \rangle = \frac{G_F}{2\sqrt{2}} V_{cd} V_{us}^* c_- \langle \mathcal{B}' | O_- | \mathcal{B} \rangle, \qquad (A.4)$$

where and $O_\pm = (\bar{d}c)(\bar{u}s) \pm (\bar{d}s)(\bar{u}c)$ and $c_\pm = c_1 \pm c_2$. The matrix element of O_+ vanishes as this operator is symmetric in color indices. The further calculation of relevant baryon matrix elements is carried out in MIT bag model (see appendix of ref. [25]), and results

---

[5]One can get the negative signs for $\Lambda_c \to N$ FFs according to eq. (6) and table I in [37], although the authors of [37] show positive signs in table IV or V. We should point out that the physical predictions in all the references listed in table 5 are insensitive to the sign of form factors.

are

$$\langle p|O_-|\Xi_c^+\rangle = -2\sqrt{\frac{2}{3}}(X_1^D + 3X_2^D), \qquad \langle n|O_-|\Xi_c^0\rangle = 2\sqrt{\frac{2}{3}}(X_1^D - 3X_2^D),$$

$$\langle p|O_-|\Xi_c'^+\rangle = -\frac{2}{3}\sqrt{2}(X_1^D - 9X_2^D), \qquad \langle n|O_-|\Xi_c'^0\rangle = \frac{2}{3}\sqrt{2}(X_1^D + 9X_2^D),$$

$$\langle \Sigma^0|O_-|\Omega_c^0\rangle = \frac{4}{3}\sqrt{2}X_1^D, \qquad \langle \Lambda^0|O_-|\Omega_c^0\rangle = -4\sqrt{6}X_2^D, \tag{A.5}$$

where we have introduced the bag integrals X_1^D and X_2^D as

$$X_1^D = \int_0^R r^2 dr(u_u v_u - v_u u_u)(u_c v_s - v_c u_s),$$

$$X_2^D = \int_0^R r^2 dr(u_u u_u + v_u v_u)(u_c u_s + v_c v_s), \tag{A.6}$$

with the numbers $X_1^D = 0, X_2^D = 1.78 \times 10^{-4}$. To obtain numerical results, we have employed the following bag parameters

$$m_u = m_d = 0, \quad m_s = 0.279 \text{ GeV}, \quad m_c = 1.551 \text{ GeV}, \quad R = 5 \text{ GeV}^{-1}, \tag{A.7}$$

where R is the radius of the bag.

A.3 Axial-vector form factors

Here we directly show the results of MIT bag model estimation of axial-vector form factors,

$$-2g_{\Xi_c'^+\Xi^+}^{A(\eta_8)} = \frac{6}{5}g_{PP}^{A(\pi^0)} = -2\sqrt{3}g_{\Xi_c'^+\Xi^+}^{A(\pi^0)} = \frac{3}{5}g_{np}^{A(\pi^+)} = -\sqrt{3}g_{\Xi_c'^0\Xi_c^+}^{A(\pi^+)} = -2g_{\Xi_c'^0\Xi_c^0}^{A(\eta_8)}$$

$$= -\frac{6}{5}g_{nn}^{A(\pi^0)} = 2\sqrt{3}g_{\Xi_c'^0\Xi_c^0}^{A(\pi^0)} = \frac{3}{5}g_{Pn}^{A(\pi^-)} = -\sqrt{3}g_{\Xi_c'^+\Xi^0}^{A(\pi^-)} = 2\sqrt{3}g_{PP}^{A(\eta_8)}$$

$$= 2\sqrt{3}g_{nn}^{A(\eta_8)} = (4\pi)Z_1, \tag{A.8}$$

$$3\sqrt{2}g_{\Sigma^0 P}^{A(K^+)} = -\frac{\sqrt{6}}{3}g_{\Lambda^0 P}^{A(K^+)} = 3g_{\Sigma^+ P}^{A(K^0)} = 3g_{\Sigma^- n}^{A(K^+)} = -\frac{\sqrt{6}}{2}g_{\Omega_c^0\Xi_c^0}^{A(K^0)}$$

$$= -\frac{\sqrt{6}}{3}g_{\Lambda^0 n}^{A(K^0)} = -\sqrt{3}g_{\Xi_c'^+\Lambda_c^+}^{A(K^0)} = -\frac{\sqrt{6}}{2}g_{\Omega_c^0\Xi_c^+}^{A(K^+)} = -3\sqrt{2}g_{\Sigma^0 n}^{A(K^0)}$$

$$= \sqrt{3}g_{\Xi_c'^0\Lambda_c^+}^{A(K^+)} = (4\pi)Z_2,$$

$$g_{\Xi_c^+\Xi^+}^{A(\eta_8)} = g_{\Xi_c^+\Xi_c^+}^{A(\pi^0)} = g_{\Xi_c^0\Xi_c^+}^{A(\pi^+)} = g_{\Xi^-\Xi_c^+}^{A(K^+)} = g_{\Xi_c^0\Xi_c^0}^{A(\eta_8)} = g_{\Xi_c^0\Xi_c^0}^{A(\pi^0)} = g_{\Xi_c^0\Lambda_c^+}^{A(K^+)}$$

$$= g_{\Xi_c^+\Xi_c^0}^{A(\pi^-)} = g_{\Xi_c^+\Lambda_c^+}^{A(K^0)} = 0,$$

where the auxiliary bag integrals are given by

$$Z_1 = \int r^2 dr \left(u_u^2 - \frac{1}{3}v_u^2\right), \qquad Z_2 = \int r^2 dr \left(u_u u_s - \frac{1}{3}v_u v_s\right). \tag{A.9}$$

Numerically, $(4\pi)Z_1 = 0.65$ and $(4\pi)Z_2 = 0.71$. Our results in the last equation also confirm the vanishing coupling between antritriplet baryons.

References

[1] Belle collaboration, *Measurement of the branching fraction* $\mathcal{B}(\Lambda_c^+ \to pK^-\pi^+)$, *Phys. Rev. Lett.* **113** (2014) 042002 [arXiv:1312.7826] [InSPIRE].

[2] BESIII collaboration, *Measurements of absolute hadronic branching fractions of* Λ_c^+ *baryon*, *Phys. Rev. Lett.* **116** (2016) 052001 [arXiv:1511.08380] [InSPIRE].

[3] Particle Data Group collaboration, *Review of particle physics*, *Phys. Rev. D* **98** (2018) 030001 [InSPIRE].

[4] BESIII collaboration, *Evidence for the singly-Cabibbo-suppressed decay* $\Lambda_c^+ \to p\eta$ *and search for* $\Lambda_c^+ \to p\pi^0$, *Phys. Rev. D* **95** (2017) 111102 [arXiv:1702.05279] [InSPIRE].

[5] Belle collaboration, *First measurements of absolute branching fractions of the* Ξ_c^0 *baryon at Belle*, *Phys. Rev. Lett.* **122** (2019) 082001 [arXiv:1811.09738] [InSPIRE].

[6] Belle collaboration, *First measurements of absolute branching fractions of the* Ξ_c^+ *baryon at Belle*, *Phys. Rev. D* **100** (2019) 031101 [arXiv:1904.12093] [InSPIRE].

[7] LHCb collaboration, *Observation of new* Ξ_c^0 *baryons decaying to* $\Lambda_c^+ K^-$, *Phys. Rev. Lett.* **124** (2020) 222001 [arXiv:2003.13649] [InSPIRE].

[8] BESIII collaboration, *Future physics programme of BESIII*, *Chin. Phys. C* **44** (2020) 040001 [arXiv:1912.05983] [InSPIRE].

[9] LHCb collaboration, *Precision measurement of the* Λ_c^+, Ξ_c^+ *and* Ξ_c^0 *baryon lifetimes*, *Phys. Rev. D* **100** (2019) 032001 [arXiv:1906.08350] [InSPIRE].

[10] C.Q. Geng, C.-W. Liu and T.-H. Tsai, *Asymmetries of anti-triplet charmed baryon decays*, *Phys. Lett. B* **794** (2019) 19 [arXiv:1902.06189] [InSPIRE].

[11] C.Q. Geng, C.-W. Liu and T.-H. Tsai, *Updated results of charmed baryon decays with* SU(3) *flavor symmetry*, talk given at the *Charm physics workshop*, November 22–24, Guangzhou, China (2019).

[12] H.J. Zhao, Y.-L. Wang, Y.K. Hsiao and Y. Yu, *A diagrammatic analysis of two-body charmed baryon decays with flavor symmetry*, *JHEP* **02** (2020) 165 [arXiv:1811.07265] [InSPIRE].

[13] L.-L. Chau, H.-Y. Cheng and B. Tseng, *Analysis of two-body decays of charmed baryons using the quark diagram scheme*, *Phys. Rev. D* **54** (1996) 2132 [hep-ph/9508382] [InSPIRE].

[14] J.G. Korner and M. Krämer, *Exclusive nonleptonic charm baryon decays*, *Z. Phys. C* **55** (1992) 659 [InSPIRE].

[15] M.A. Ivanov, J.G. Korner, V.E. Lyubovitskij and A.G. Rusetsky, *Exclusive nonleptonic decays of bottom and charm baryons in a relativistic three quark model: evaluation of nonfactorizing diagrams*, *Phys. Rev. D* **57** (1998) 5632 [hep-ph/9709372] [InSPIRE].

[16] Q.P. Xu and A.N. Kamal, *Cabibbo favored nonleptonic decays of charmed baryons*, *Phys. Rev. D* **46** (1992) 270 [InSPIRE].

[17] H.-Y. Cheng and B. Tseng, *Nonleptonic weak decays of charmed baryons*, *Phys. Rev. D* **46** (1992) 1042 [*Erratum ibid.* **55** (1997) 1697] [INSPIRE].

[18] H.-Y. Cheng and B. Tseng, *Cabibbo allowed nonleptonic weak decays of charmed baryons*, *Phys. Rev. D* **48** (1993) 4188 [hep-ph/9304286] [INSPIRE].

[19] P. Zenczykowski, *Nonleptonic charmed baryon decays: symmetry properties of parity violating amplitudes*, *Phys. Rev. D* **50** (1994) 5787 [INSPIRE].

[20] K.K. Sharma and R.C. Verma, *A study of weak mesonic decays of Λ_c and Ξ_c baryons on the basis of HQET results*, *Eur. Phys. J. C* **7** (1999) 217 [hep-ph/9803302] [INSPIRE].

[21] CLEO collaboration, *Measurement of the decay asymmetry parameters in $\Lambda_c^+ \to \Lambda\pi^+$ and $\Lambda_c^+ \to \Sigma^+\pi^0$*, *Phys. Lett. B* **350** (1995) 256 [hep-ex/9502004] [INSPIRE].

[22] P. Zenczykowski, *Quark and pole models of nonleptonic decays of charmed baryons*, *Phys. Rev. D* **50** (1994) 402 [hep-ph/9309265] [INSPIRE].

[23] A. Datta, *Nonleptonic two-body decays of charmed and Lambda(b) baryons*, hep-ph/9504428 [INSPIRE].

[24] BESIII collaboration, *Measurements of weak decay asymmetries of $\Lambda_c^+ \to pK_S^0$, $\Lambda\pi^+$, $\Sigma^+\pi^0$, and $\Sigma^0\pi^+$*, *Phys. Rev. D* **100** (2019) 072004 [arXiv:1905.04707] [INSPIRE].

[25] H.-Y. Cheng, X.-W. Kang and F. Xu, *Singly Cabibbo-suppressed hadronic decays of Λ_c^+*, *Phys. Rev. D* **97** (2018) 074028 [arXiv:1801.08625] [INSPIRE].

[26] J. Zou, F. Xu, G. Meng and H.-Y. Cheng, *Two-body hadronic weak decays of antitriplet charmed baryons*, *Phys. Rev. D* **101** (2020) 014011 [arXiv:1910.13626] [INSPIRE].

[27] H.-Y. Cheng, G. Meng, F. Xu and J. Zou, *Two-body weak decays of doubly charmed baryons*, *Phys. Rev. D* **101** (2020) 034034 [arXiv:2001.04553] [INSPIRE].

[28] S. Hu, G. Meng and F. Xu, *Hadronic weak decays of the charmed baryon Ω_c*, *Phys. Rev. D* **101** (2020) 094033 [arXiv:2003.04705] [INSPIRE].

[29] P.-Y. Niu, J.-M. Richard, Q. Wang and Q. Zhao, *Hadronic weak decays of Λ_c in the quark model*, *Phys. Rev. D* **102** (2020) 073005 [arXiv:2003.09323] [INSPIRE].

[30] A. Chodos, R.L. Jaffe, K. Johnson and C.B. Thorn, *Baryon structure in the bag theory*, *Phys. Rev. D* **10** (1974) 2599 [INSPIRE].

[31] T.A. DeGrand, R.L. Jaffe, K. Johnson and J.E. Kiskis, *Masses and other parameters of the light hadrons*, *Phys. Rev. D* **12** (1975) 2060 [INSPIRE].

[32] G. Buchalla, A.J. Buras and M.E. Lautenbacher, *Weak decays beyond leading logarithms*, *Rev. Mod. Phys.* **68** (1996) 1125 [hep-ph/9512380] [INSPIRE].

[33] T. Feldmann, P. Kroll and B. Stech, *Mixing and decay constants of pseudoscalar mesons: The Sequel*, *Phys. Lett. B* **449** (1999) 339 [hep-ph/9812269] [INSPIRE].

[34] T. Feldmann, P. Kroll and B. Stech, *Mixing and decay constants of pseudoscalar mesons*, *Phys. Rev. D* **58** (1998) 114006 [hep-ph/9802409] [INSPIRE].

[35] D. Fakirov and B. Stech, *F and D decays*, *Nucl. Phys. B* **133** (1978) 315 [INSPIRE].

[36] R. Perez-Marcial, R. Huerta, A. Garcia and M. Avila-Aoki, *Predictions for Semileptonic Decays of Charm Baryons. 2. Nonrelativistic and MIT bag quark models*, *Phys. Rev. D* **40** (1989) 2955 [*Erratum ibid.* **44** (1991) 2203] [INSPIRE].

[37] Z.-X. Zhao, *Weak decays of heavy baryons in the light-front approach*, *Chin. Phys. C* **42** (2018) 093101 [`arXiv:1803.02292`] [INSPIRE].

[38] R.N. Faustov and V.O. Galkin, *Semileptonic decays of Λ_c baryons in the relativistic quark model*, *Eur. Phys. J. C* **76** (2016) 628 [`arXiv:1610.00957`] [INSPIRE].

[39] T. Gutsche, M.A. Ivanov, J.G. Körner, V.E. Lyubovitskij and P. Santorelli, *Heavy-to-light semileptonic decays of Λ_b and Λ_c baryons in the covariant confined quark model*, *Phys. Rev. D* **90** (2014) 114033 [*Erratum ibid.* **94** (2016) 059902] [`arXiv:1410.6043`] [INSPIRE].

[40] C.-F. Li, Y.-L. Liu, K. Liu, C.-Y. Cui and M.-Q. Huang, *Analysis of the semileptonic decay $\Lambda_c \to n e^+ \nu_e$*, *J. Phys. G* **44** (2017) 075006 [`arXiv:1610.05418`] [INSPIRE].

[41] A. Khodjamirian, C. Klein, T. Mannel and Y.-M. Wang, *Form factors and strong couplings of heavy baryons from QCD light-cone sum rules*, *JHEP* **09** (2011) 106 [`arXiv:1108.2971`] [INSPIRE].

[42] S. Meinel, *$\Lambda_c \to N$ form factors from lattice QCD and phenomenology of $\Lambda_c \to n \ell^+ \nu_\ell$ and $\Lambda_c \to p \mu^+ \mu^-$ decays*, *Phys. Rev. D* **97** (2018) 034511 [`arXiv:1712.05783`] [INSPIRE].